

Crosslink between lipids and acute uveitis: a lipidomic analysis

Hai-Yan Wang^{1,2,3}, Yi Wang^{4,5}, Yuan Zhang^{1,2,3}, Jing Wang^{1,2,3}, Shu-Yu Xiong^{1,2,3}, Qian Sun^{1,2,3}

¹Department of Ophthalmology, Shanghai First People's Hospital Affiliated to Jiaotong University, Shanghai 200080, China

²Shanghai Key Laboratory of Ocular Fundus Disease, Shanghai 200080, China

³Shanghai Engineering Center for Visual Science and Photomedicine, Shanghai 200080, China

⁴Department of Chemistry, Fudan University, Shanghai 200030, China

⁵Department of Institutes of Biomedical Sciences, Fudan University, Shanghai 200030, China

Correspondence to: Qian Sun. Department of Ophthalmology, Shanghai First People's Hospital Affiliated to Jiaotong University, Shanghai 200080, China. Dr_sunqian@126.com

Received: 2018-02-26 Accepted: 2018-03-15

Abstract

• **AIM:** To explore the roles of phospholipids and sphingolipids in the inflammatory process of uveitis.

• **METHODS:** Aqueous humor (AH) and the retina were obtained from endotoxin-induced uveitis (EIU) rats during the acute inflammation stage (24h after endotoxin injection). Lipids were extracted using a modified Bligh and Dyer method and subjected to mass spectrometric identification using class-specific lipid standards and ratiometric quantification. Relative intensity analysis was performed to evaluate the amount change of common lipids between the EIU and control groups.

• **RESULTS:** Unique lipid species encompassing all five phospholipid classes were found in both control and the EIU AH and retina. Commensurate with the significantly increased level of lysophospholipids in the EIU AH and retina, we found that the ratio of lysophospholipids to total phospholipids was significantly increased too. We also detected a significant increase in 18:0 lysophosphatidylcholine levels in the EIU group (fold change =6.4 in AH and 3.8 in retina). Cer240, Cer241, and SM240 levels remarkably increased in the EIU AH. Enhanced C12 ceramide-1-phosphate (C12 C-1-P), C16 C-1-P, C24 C-1-P, and upregulated Cer160, Cer240, SM120, and SM240 were found in EIU retina. C-1-P was believed to restore homeostasis by inhibiting nuclear factor kappa B (NF-κB) activation. However, we still found elevated NF-κB levels in the EIU retina.

• **CONCLUSION:** A variety of lipids might have played a critical role in EIU inflammation. Exogenous topical application of these protective lipids or inhibition of these pro-inflammatory lipids may be useful therapeutic strategies for the resolution of EIU.

• **KEYWORDS:** lipidomics; mass spectrometry; uveitis; phospholipid; sphingolipid

DOI:10.18240/ijo.2018.05.05

Citation: Wang HY, Wang Y, Zhang Y, Wang J, Xiong SY, Sun Q. Crosslink between lipids and acute uveitis: a lipidomic analysis. *Int J Ophthalmol* 2018;11(5):736-746

INTRODUCTION

Uveitis is considered as a relatively common intraocular inflammatory disease with a cumulative yearly incidence in the elderly averaging 340.9/100 000 persons per year in the United States. It can cause severe ocular impairments when it is misdiagnosed or when there is no timely intervention. Moreover, its intractable recurrence can even lead to cataract, glaucoma, macular edema, and total blindness^[1-3]. Unfortunately, the etiology of uveitis is still poorly understood, leading to unsatisfactory treatment. To the best of our knowledge, it is theorized to be a noninfectious, immune-mediated response. Recent studies focusing on inflammation have reported that phospholipids can participate in immunomodulation^[4]. Phospholipids, initially known as major membrane components, are now considered as bioactive signaling molecules that could mediate a variety of cellular responses, including inflammation. A variety of lysophospholipids are also believed to modulate neutrophil and macrophage activation, and phagocytic clearance of apoptotic cells^[5-8]. Thus, it might be valuable to explore the role of phospholipids in the inflammatory process of uveitis. Experimental studies have also revealed that sphingolipids, which are important signaling molecules as well as components of membranes and extracellular fluids, are also involved in stress response and inflammation^[9-12]. Several endogenous lipid mediators such as prostaglandins (PGs), leukotrienes (LTs), and tumor necrosis factor (TNF)-alpha-induced protein 8 (TNFAIP8 or TIPE) have also attracted attention in recent years for their roles in regulating inflammation and crosslinking with lipids^[13-14]. Thus, knowledge of the

signaling pathways of phospholipids, sphingolipids and lipid mediators will enhance our understanding of the molecular and cellular mechanisms underlying the inflammatory process of uveitis. This may allow the development of novel therapeutic diagnostics and approaches for sufficient treatment.

Endotoxin-induced uveitis (EIU) is established by injecting Gram-negative bacteria lipopolysaccharides (LPS) to certain strains of rodents. This is widely regarded as a stable model of human acute uveitis, and is used for mechanism exploration and innovative therapeutic drug testing^[15]. EIU has been generally considered to cause inflammation in the anterior chamber; posterior inflammation has also been reported, including choroiditis, vitritis, retinal vascular leukostasis, and inflammatory cell infiltration into vitreous mostly near the optic nerve head^[16-19]. We adopted this classical model for our study to investigate the role of lipids in the inflammatory process of uveitis.

MATERIALS AND METHODS

Ethics Statement All studies involving animals were conducted in strict accordance with the Association for Research in Vision and Ophthalmology Statement for the Use of Animals in Ophthalmic and Vision Research. The protocol was prospectively approved by the Ethics Committee of Shanghai First People's Hospital of Shanghai Jiaotong University, China. Animals used in this research received every consideration for their comfort and were properly housed and fed, with their surroundings kept in a sanitary condition. The minimal number of rat was used in the experiments. Animals used in the research were used according to the appropriateness of experimental procedures. Sodium pentobarbital anesthesia was used to eliminate sensibility to pain during all surgical procedures. Buprenorphine (0.01 mg/kg, intraperitoneal) was administered pre-operatively for preemptive analgesia and once post-operatively. Animals under anesthesia were placed on warm water circulating pads to avoid hypothermia and were closely observed every hour for heart rate, respiratory rate, body temperature, *etc.* Redness around the injection site, abnormal breathing, dehydration, unkempt appearance, decreased movement, aggressive behavior, and food and water consumption were adequately monitored by trained staff every 8h post-injection. Immediately after the sample collection from both eyes, carbon dioxide inhalation was performed for euthanasia while the experimental animals were still under anesthesia.

Establishing the Endotoxin-induced Uveitis Model Six-week-old Wistar rats (160-180 g) were obtained from Shanghai Laboratory Animal Center of the Chinese Academy of Sciences, and housed in a 12-h light/12-h dark cycle vivarium with food and water supplied *ad libitum* a week prior to the procedure. The EIU model was established by a single right foot-pad injection of 100 μ L sterilized pyrogen-free saline containing 200 μ g LPS from *Escherichia coli* (Sigma-Aldrich,

Inc., St. Louis, MO, USA). A control group was given the same volume of sterilized saline solution.

Clinical Manifestation Evaluation Slit-lamp examination was performed 24h after injection for both eyes. Clinical manifestations were evaluated according to the grading system reported previously^[12,20]: 0, no sign of inflammation; 1, discrete dilation of the iris and conjunctival vessels; 2, moderate dilation of the iris and conjunctival vessels with moderate flare in the anterior chamber; 3, intense iridal hyperemia with intense flare in the anterior chamber; 4, same signs as in 3 with presence of fibrinous exudate in the pupillary area and miosis.

Aqueous Humor Procurement Wistar rats were anesthetized by an intraperitoneal injection. A drop of tetracaine hydrochloride ophthalmic solution (0.5%, Bausch & Lomb, USA) was used to anesthetize the ocular surface prior to aqueous humor (AH) procurement. AH from the experimental and control groups was obtained from the anterior chamber of both eyes through paracentesis using a syringe (catalog No.7635-01 Hamilton, Reno, Nevada) with a small 33-gauge removable needle (701RN, catalog No.7803-05 Hamilton). A total of 24 to 30 μ L AH was collected per rat (12-15 μ L/eye) and used for subsequent analysis. After AH procurement, the retina of each eye was isolated carefully for Western blot analysis.

Infiltrating Cell Counting and Protein Concentration Detection For cell counting, the sample was suspended in an equal amount of Türk's stain solution, and the cell counting per field was performed by two independent researchers using a hemocytometer under a light microscope. The total cell number per microliter was calculated by averaging the values of four fields from each sample. The total protein concentration was measured by NanoDrop 2000/2000c spectrophotometer (ThermoFisher, MA, USA).

Hematoxylin and Eosin Staining Hematoxylin and eosin (HE) staining of the anterior chamber and retina of both eyes was performed 24h after LPS stimulation. The eyes were enucleated and fixed in 4% paraformaldehyde for 20h, incubated in 20% sucrose, and then embedded in paraffin. Subsequently, fixed eyes were sectioned at a thickness of 5 μ m and then stained with hematoxylin and eosin solution (Sigma). An Axioplan 2 imaging microscope (Zeiss, Jena, Germany) was used for histological evaluation of the sections, and color micrographs were obtained at 5 \times and 400 \times magnification using Zeiss Axiovision software (Zeiss).

Enzyme-linked Immunosorbent Assay The acquired AH ($n=3$ per group) were centrifuged at 2500 rpm for 20min to obtain the supernatant. The protein levels of tumor necrosis factor-alpha (TNF- α) and interleukin-6 (IL-6) were measured using the rat TNF- α and IL-6 enzyme-linked immunosorbent assay (ELISA) kit (R&D Systems, Minneapolis, MN, USA) according to the manufacturer's instruction. The minimum detectable doses of rat TNF- α and IL-6 are approximately 5.0 pg/mL and 22.0 pg/mL, respectively.

Table 1 Parameters for MS/MS scan

| Mode | Optimum ESI conditions | | | Needle voltage (V) | Temperature (°C) | Declustering potential (V) | Collision energy (eV) | Dwell time (ms) |
|----------|------------------------|-------|-------|--------------------|------------------|----------------------------|-----------------------|-----------------|
| | Curtain gas | Gas 1 | Gas 2 | | | | | |
| Positive | 20 | 20 | 20 | 5500 | 450.0 | 80 | 20 to 50 | 20 |
| Negative | 20 | 20 | 20 | -4500 | 450.0 | -100 | -25 to -100 | 20 |

ESI: Electrospray ionization.

Western Blot The protein level of the inflammatory mediator nuclear factor kappa B (NF- κ B) subunit p65 in the retina of both eyes was analyzed by Western blot. Approximately 50 μ g of protein from each retina was loaded onto a 4% to 20% gradient gel along with a Sea Blue Plus 2 (Invitrogen Corporation, Carlsbad, CA, USA) protein marker, immunoblotted to a polyvinylidene fluoride membrane (Millipore, Billerica, MA, USA), and subsequently probed with NF- κ B antibody (Cell Signaling Technology Inc., Beverly, MA, USA). Coomassie Blue staining of the gel was used to demonstrate the equal protein amount loading.

Lipid Extraction A total of 24 to 30 μ L of AH was collected per rat and used for phospholipid extraction using a modified version of the Bligh and Dyer extraction method^[21-22]. Phospholipids extracted in the lower organic phase were dried using a Speed-Vac (Model 7810014; Labconco, Kansas City, MO, USA), and then flushed with argon gas for oxidation prevention. Proteins procured from the upper aqueous phase were quantified using a suitable modification of Bradford's method.

Mass Spectrometric Analysis Identification and quantification of sphingolipids and phospholipids: phosphatidylcholines (PCs), phosphatidylethanolamines (PEs), phosphatidylserines (PSs), phosphatidylinositols (PIs), and phosphatidylglycerols (PGs), and lysophospholipids:lysophosphatidylcholines (LysoPCs), lysophosphatidylethanolamines (LysoPEs), lysophosphatidylserines (LysoPSs), lysophosphatidylinositols (LysoPIs), and lysophosphatidylglycerol (LysoPGs), were performed by the mass spectrometer model QTRAP[®] 4000 (ABSciex, Canada) coupled to a liquid chromatographic (LC) system (Shimadzu, Japan), which was a LC20AB pump (Shimadzu, Japan) equipped with an SIL-20AC auto-sampler (Shimadzu, Japan). System control and data processing were performed using the Analyst 1.6 and MultiQuant 3.0 software (SCIEX, Canada), respectively.

First, the lipids separation was achieved by this LC system using a reverse phase chromatograph (RP-LC) and a normal phase chromatograph (NP-LC). The reverse phase separation was performed at room temperature (22°C) on a 2.1 \times 250-mm², Ultimate[®] AQ-C18 100 Å pore size column, 5- μ m particle size (Welch, China). Eluent A (20 mmol/L ammonium acetate in H₂O) and eluent B (20 mmol/L ammonium acetate in MeOH) were used in the gradient elution program: 0min, 75% B; 22min, 99% B; 39min, 99% B; 39.1min, 75% B; 45min, 75% B. The flow rate was set to 300 μ L/min and 10- μ L sample

volumes were injected each time. Normal phase separation was performed at room temperature (22°C) on a 2.1 \times 250-mm, Ultimate[®] SiO₂ 100 Å pore size column, 5- μ m particle size (Welch, China). Eluent A (mixture of IPA/Hexane/100 mmol/L ammonium acetate, 58/40/2, v/v/v) and eluent B (mixture of IPA/Hexane/100 mmol/L ammonium acetate, 50/40/10, v/v/v) were used for the gradient elution program: 0min, 50% B; 5min, 50% B; 30min, 100% B; 40min, 100% B; 41min, 50% B; 50min, 50% B. The flow rate and injected sample volumes were the same as those used in reverse phase separation.

After separation, lipid extracts were analyzed by QTRAP[®] 4000 operated in multiple reaction monitoring (MRM) mode. Analyses were achieved in the negative modes (LysoPIs, PIs, LysoPGs, PGs, LysoPSs, PSs, ceramide 1-phosphate, dihydroceramide 1-phosphate, sulfatide) and positive modes (LysoPCs, PCs, LysoPEs, PEs, PGs, PSs, Ceramide, ceramide 1-phosphate, sphingomyelin, sphingosine 1-phosphate, sphinganine 1-phosphate), respectively (Table 1). Total MS/MS experiments were performed by 257 positive and 300 negative MRM scans.

Data Analysis Peak identifications were performed using Multiquant software (SCIEX) and were reviewed carefully by two independent observers. Mass spectrometric data was imported into the MZmine 2.9 program, analyzed using a database downloaded from LipidMaps (www.lipidmaps.org), and then subjected to ratiometric quantification in two steps according to established procedures in previous studies^[22-23]. Only peaks that showed >2% intensity and a signal-to-noise ratio (S/N) >10 were selected. The peak intensities were processed by normalization to total signal intensities and total protein quantity. Isotopic peak correction was performed with a mass tolerance of \pm 0.5 m/z, and a maximum charge of 1. Quantitation was performed by internal standards per lipid class, and peak changes between samples were confirmed by manual quantification. All unique lipid amounts (amount of lipid species μ g/ μ g protein) were subjected to a sample *t*-test compared to 0.0 and were considered significantly different if the results indicated a $P \leq 0.05$. For common lipids from both control and EIU groups, relative intensity analysis (EIU/control) was performed to obtain fold change. The mean \pm SD of 3 independent fold changes was subsequently calculated. Values higher than 1.5 or lower than 0.67 were considered to have a significant difference.

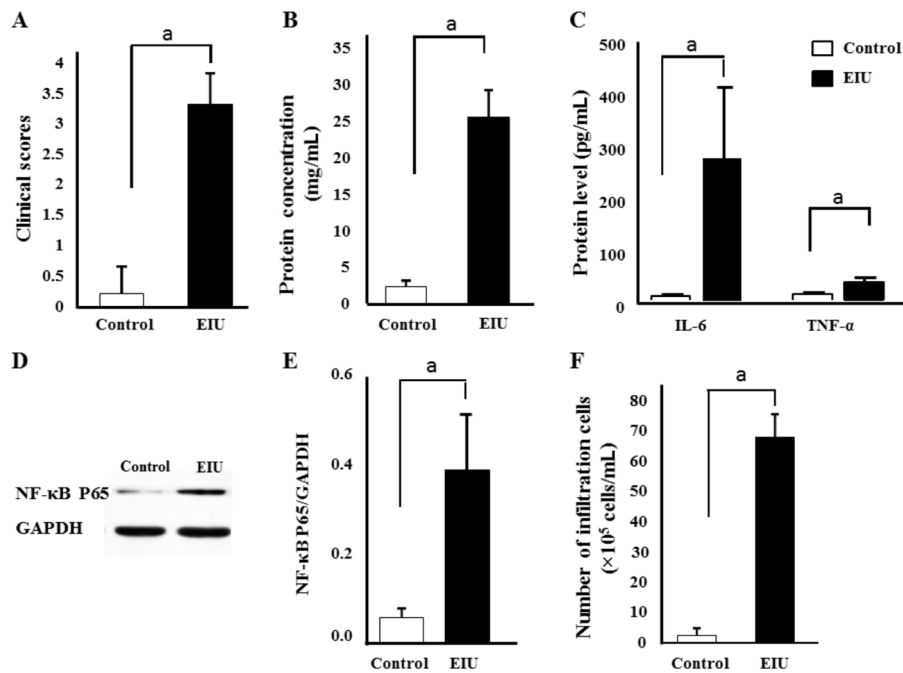


Figure 1 Establishment of the EIU model The rats were evaluated 24h after LPS stimulation. Clinical scores (A) were graded in a blinded style. Total AH protein concentration (B) and protein level of AH TNF- α and IL-6 (C) were assessed 24h after LPS injection. Protein level of retina NF- κ B P65 were measured using Western blot (D) and NF- κ B P65/GAPDH was also presented (E). Infiltrating cell counts were conducted six in AH 24h after LPS challenge (F). The results are expressed as mean \pm SD from three independent experiments. ^a P \leq 0.01.

Statistical Analysis Data are expressed as mean \pm SD of at least three independent experiments. Severity of EIU was analyzed using the nonparametric Mann-Whitney U test. A P -value of less than 0.05 was considered statistically significant. All computations were performed with SPSS16.0 (Chicago, IL, USA) software.

RESULTS

Establishment of Endotoxin-induced Uveitis No signs of uveitis were observed in the sterile saline control group. Severe inflammation was noticed 24h after LPS administration in EIU group. The clinical score of these EIU rats was 3.33 (Figure 1A), with intense flare in the anterior chamber, and even fibrinous exudate in the pupillary area. Soluble protein measurement showed high concentration (25.62 mg/mL) (Figure 1B). Very low levels of IL-6 and TNF- α were detected in the control AH. In contrast, remarkably upregulated IL-6 and TNF- α were found in the EIU AH 24h after injection (Figure 1C). NF- κ B level in EIU retina was significantly elevated compared to that in the control retina (P <0.05; Figure 1D and 1E). Massive amounts of leukocytes presented in the EIU anterior chamber (67×10^5 cells/mL; Figure 1F). Subsequent histological evaluation showed numerous neutrophils and monocytes in the EIU anterior chamber (Figure 2C). Massive exudation and a relatively small number of neutrophils and monocytes were observed in EIU posterior vitreous (Figure 2D). No leukocyte infiltration was discovered in the anterior chamber (Figure 2A) and posterior vitreous (Figure 2B) from the control group.

Aqueous Humor Lipid Changes Between the Control and Endotoxin-induced Uveitis Groups A slight increase in total

sphingolipids and phospholipids was observed in the EIU AH compared to that in control AH, which was due to remarkably decreased total PS and PE, and significantly increased PC, PI, and PG (Figure 3A). For each class, structural comparisons between the EIU and control groups were conducted and a variety of lipids were found to be common or unique to the control and EIU groups. The numbers of total, common and unique lipids in each group are presented in Figure 3B. There were 1 unique PS and 3 unique PEs in the control group that were below the detection limit in the EIU group, and 8 unique PCs, 2 unique PEs, 6 unique PIs, and 2 unique PGs in the EIU group that were undetectable in the control group. Considering these common lipids, relative intensity analysis was performed and the most common lipids showed differences between these two groups (Figures 3C and 4). It is worth mentioning that Cer240, Cer241, and SM240 remarkably increased in the EIU AH by 1.6-, 9.0-, and 2.0-fold, respectively (Figure 4D).

Lysophospholipids are formed from phospholipids when tissues are subjected to stress or are under elevated hydrolytic conditions. The relative intensity comparison of lysophospholipid species was performed; a significant increase in total lysophospholipids was found in the EIU AH compared to that in the control AH (Figure 5A). Interestingly, only the LysoPS showed a significant decrease (fold change=0.37), while the other four lysophospholipid species (LysoPC, LysoPE, LysoPI, and LysoPG) showed a remarkable increase (fold change >1.5) in the EIU group (Figure 5A). We also determined the ratio of lysophospholipids to total phospholipids in both groups. Commensurate with the increase in the amount of

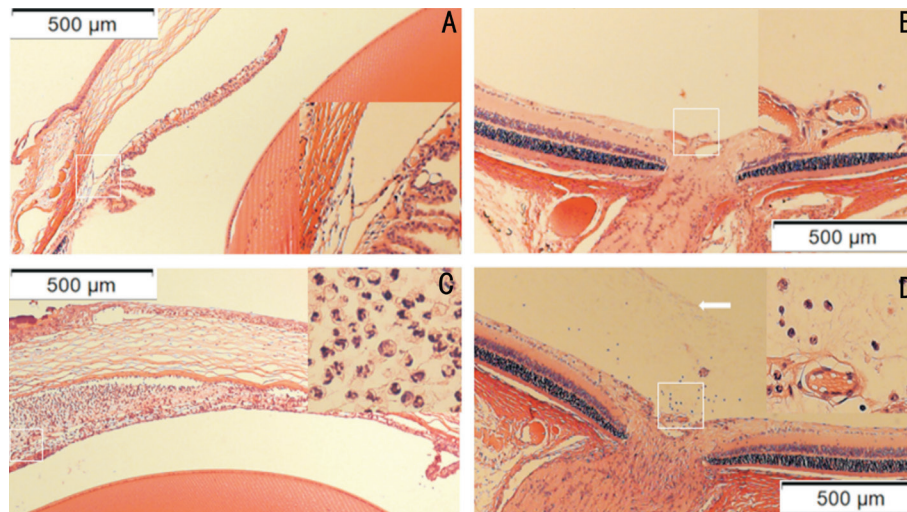


Figure 2 Histological assessment of the EIU model HE staining of the anterior chamber and retina was performed 24h after LPS stimulation. No signs of inflammation was observed in the control AH (A) and retina (B). On the contrary, numerous neutrophils and monocytes presented in the EIU anterior chamber (C). Massive exudation (arrow) and relative little amount neutrophils and monocytes were found in the EIU posterior vitreous (D).

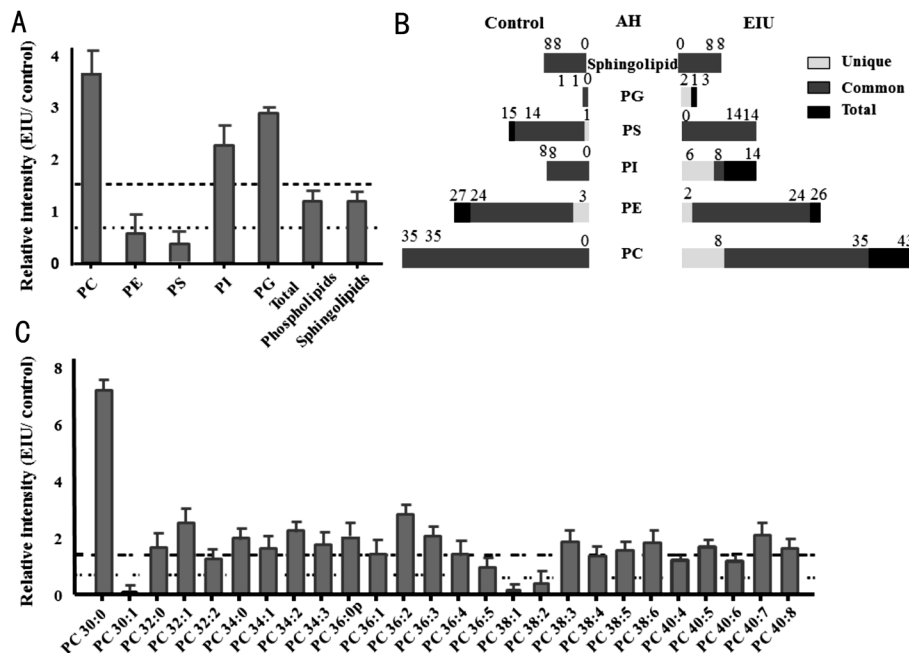


Figure 3 Relative intensity analysis of total lipid and common PC species between the EIU and control AH and total species counts (unique, common and total) A: Relative intensity analysis of total sphingolipids and phospholipids of PC, PE, PS, PI and PG, was conducted (the ratio of EIU to control AH); B: The number of common, unique, and total sphingolipid and phospholipid species was presented as indicated in control and the EIU AH; C: Relative intensity analysis of common PC species was performed (the ratio of EIU to control AH). Dashed line indicates a relative intensity =1.5; Dotted line indicates a relative intensity =0.67.

phospholipids, the ratio of total lysophospholipids to total phospholipids was also considerably increased in the EIU AH compared to that in the control group (Figure 5B). All five lysophospholipid subspecies, including LysoPC, LysoPE, LysoPS, LysoPI, and LysoPG, also had increased levels in the EIU AH. LysoPC and LysoPE contributed major increases among all five classes. It is noteworthy that LysoPS in the inflammatory group showed a slight increase (2%) in ratio even though the amount reduced as stated above.

Retina Lipid Changes Between the Control and Endotoxin-induced Uveitis Groups We observed a remarkable increase

in total sphingolipids and phospholipids, including PC, PE, PS, PI, and PG in the EIU retina compared to that in the control retina (Figure 6A). The number of total, common, and unique lipids in each group is also presented in Figure 6B. There was only 1 unique PS in the control group; 3 unique PSs, 5 unique PIs, 4 unique PGs, and 1 unique DHC1P240 were exclusively produced in the EIU group. The relative intensity analysis of common lipids demonstrated that most common lipids showed differences in amount between EIU and control groups (Figures 6C, 7, and 8). We would like to emphasize that the amount of total sphingolipids also significantly increased in

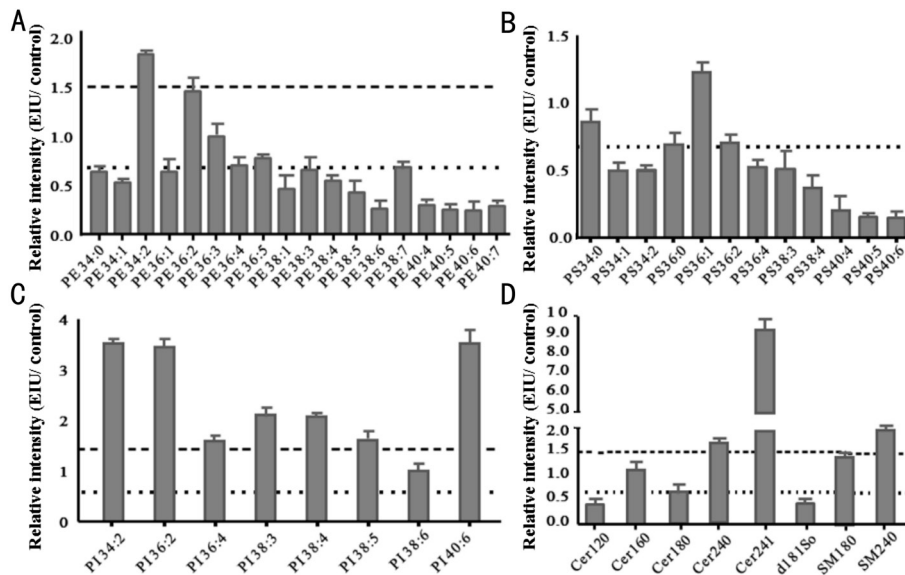


Figure 4 Relative intensity analysis of common PE, PS, PI, and sphingolipid species between the EIU and control AH A: Relative intensity analysis of common PE species (the ratio of EIU to control AH); B: Relative intensity analysis of common PS species (the ratio of EIU to control AH); C: Relative intensity analysis of common PI species (the ratio of EIU to control AH); D: Relative intensity analysis of common sphingolipid species (the ratio of EIU to control AH). Dashed line indicates a relative intensity =1.5; Dotted line indicates a relative intensity =0.67.

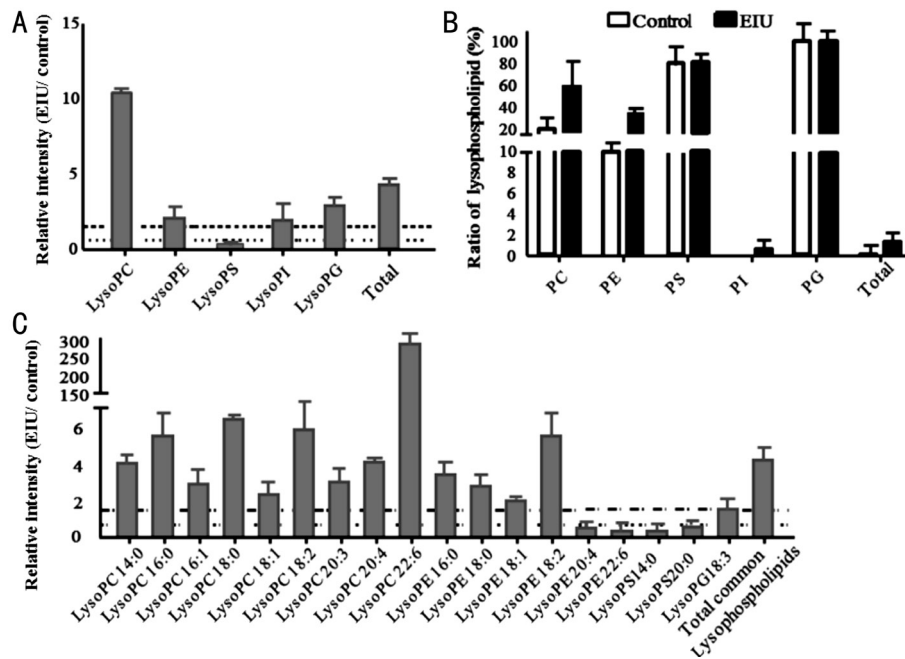


Figure 5 Relative intensity analysis of common lysophospholipid species between the EIU and control AH and the percentage of lysophospholipids to phospholipids A: Relative intensity analysis of total lysophospholipids (the ratio of EIU to control AH); B: Summary of the percentage of lysophospholipid to the phospholipid is as indicated each bar for that lipid class; C: Relative intensity analysis of common lysophospholipid species (the ratio of EIU to control AH). Dashed line indicates a relative intensity =1.5; Dotted line indicates a relative intensity =0.67.

the EIU retina by 2.8-fold. In addition, increased C12 ceramide-1-phosphate (C-1-P), C16 C-1-P, C24 C-1-P, upregulated Cer160, Cer240, SM120, and SM240 were also found in the EIU retina (Figure 8C).

The relative intensity measurement of lysophospholipid species were conducted and a significant increase in total lysophospholipids, and all 5 classes including LysoPC, LysoPE, LysoPS, LysoPI, and LysoPG were presented in Figure 9A. We also determined the level of lysophospholipids to total phospholipids in both groups respectively. Consistent with the amount increase, the ratio of total lysophospholipids to total

phospholipids is also considerably higher in the inflammatory state than the normal state (Figure 9B). Relative intensity analysis of common lysophospholipids from each class was performed too and most of them show significant difference in amount. Data derived from our study showed noteworthy increase in 18:0 LysoPC in the EIU group (fold change=3.8). 18:0 and 18:1 LysoPS, already known as bioactive signaling phospholipids, showed a significant enhancement in the EIU retina by 2.9- and 1.6-fold respectively over that in control retina (Figure 9C).

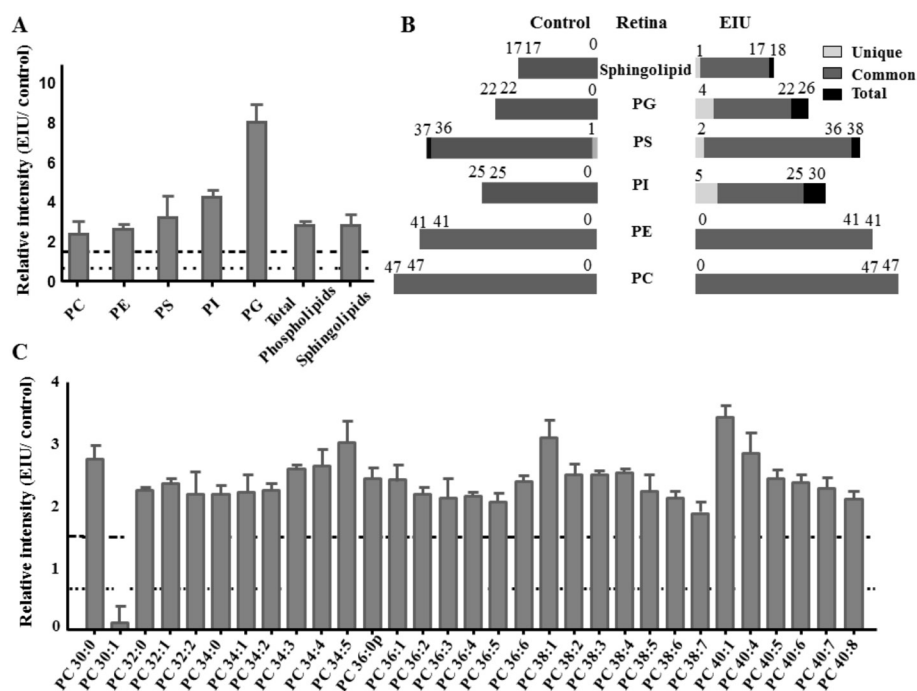


Figure 6 Relative intensity analysis of total lipid and common PC species between the EIU and control retina and total species counts (unique, common and total) A: Relative intensity analysis of total sphingolipids and phospholipids of all five classes: PC, PE, PS, PI and PG; B: The number of total, common, and unique sphingolipid and phospholipid species as indicated in control and EIU retina; C: Relative intensity analysis of common PC species (the ratio of EIU to control retina). Dashed line indicates a relative intensity =1.5; Dotted line indicates a relative intensity =0.67.

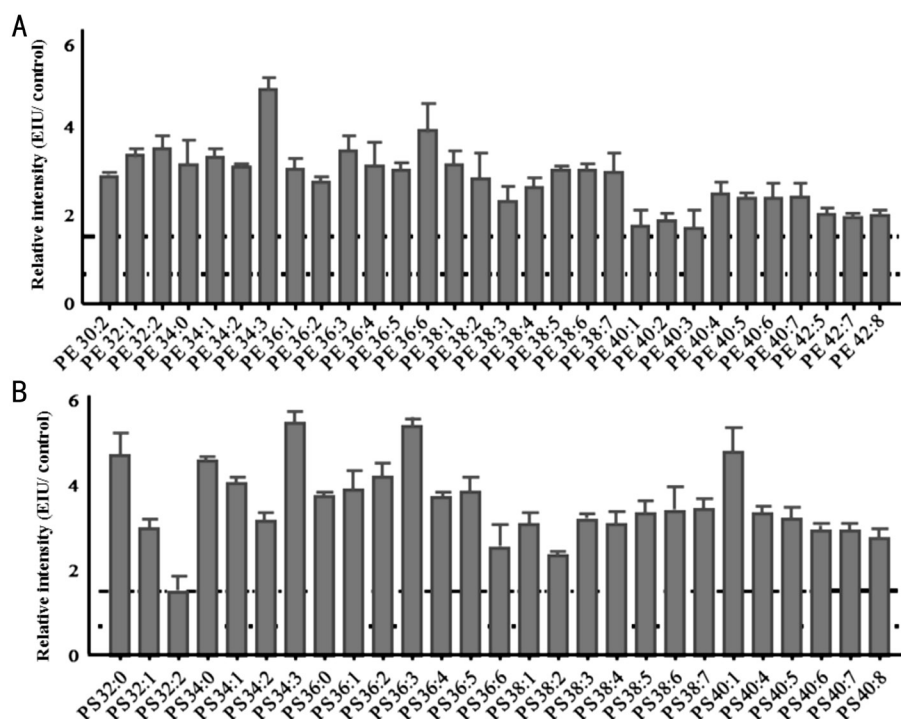


Figure 7 Relative intensity analysis of common PE and PS species between the EIU and control retina A: Relative intensity analysis of common PE species (the ratio of EIU to control retina); B: Relative intensity analysis of common PS species (the ratio of EIU to control retina). Dashed line indicates a relative intensity =1.5; Dotted line indicates a relative intensity =0.67.

DISCUSSION

In this study, we found an increase in total phospholipids in the EIU AH, with remarkably decreased total PS and PE, and significantly increased PC, PI, PG, and sphingolipids. In addition, an increase in total phospholipids and all the six

classes, including PC, PE, PS, PI, PG, and sphingolipids was also discovered in the EIU retina. For both the AH and retina, PI increased due to acute inflammation, and 5 unique PIs (PI 14:0/22:6, PI 18:1/20:0, PI 18:1/22:0, LysoPI 16:0, and LysoPI 18:0) were detected exclusively in the EIU group.

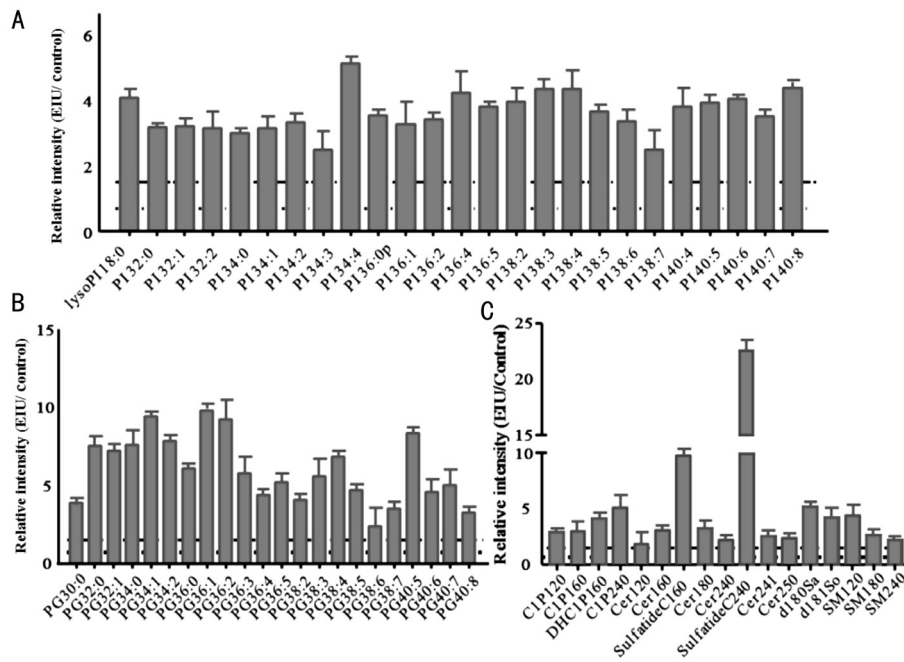


Figure 8 Relative intensity analysis of common PI, PG, and sphingolipid species between the EIU and control retina A: Relative intensity analysis of common PI species (the ratio of EIU to control retina); B: Relative intensity analysis of common PG species (the ratio of EIU to control retina); C: Relative intensity analysis of common sphingolipid species (the ratio of EIU to control retina). Dashed line indicates a relative intensity =1.5; Dotted line indicates a relative intensity =0.67.

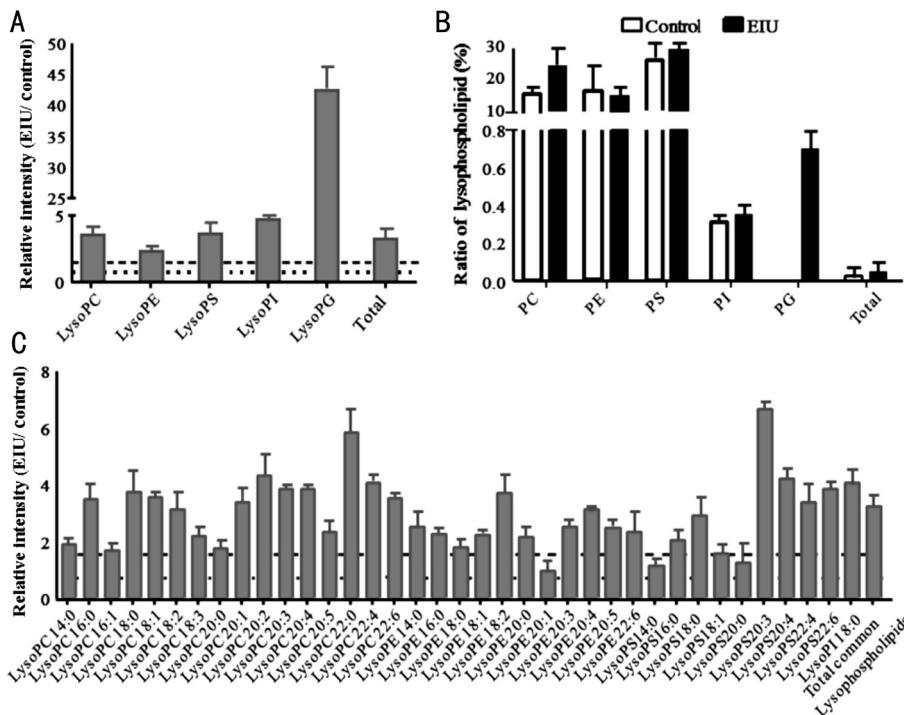


Figure 9 Relative intensity analysis of total lysophospholipid and common lysophospholipid species between the EIU and control retina and the percentage of lysophospholipids to phospholipids A: Relative intensity analysis of total lysophospholipids (the ratio of EIU to control retina); B: The percentage of lysophospholipid to the phospholipid is as indicated above each bar for that lipid class; C: Relative intensity analysis of common lysophospholipid species (the ratio of EIU to control retina). Dashed line indicates a relative intensity =1.5. Dotted line indicates a relative intensity =0.67.

As referenced in several studies, PIs can interact with a protein from the TNFAIP8 family, designated TIPE2, a newly identified negative mediator of Toll-like receptor (TLR), which plays a critical role in regulating both innate and adaptive immunity and maintaining immune

homeostasis^[4,13,24]. Hypothetically, the PI enhancement in EIU might be the attempt to tightly control the strength and duration of the immune response, prevent hyper-responsiveness to inflammation, and reduce the chance of tissue injury.

In comparison with the control group, the relative intensity analysis of common PGs showed a noteworthy increase in the EIU AH by 1.5-fold and the EIU retina by 8.0-fold. 2 LysoPGs (LysoPG 18:0, LysoPG 20:3) were uniquely detected in the EIU AH, and 3 LysoPGs (LysoPG 18:0, LysoPG 20:3, and LysoPG 22:6) and 1 PG (PG 34:3) were found exclusively in the EIU retina. Similar results were also found in several chronic disease, such as osteoarthritis and rheumatoid arthritis^[25]. PGs have been described as the pro-inflammatory lipid mediators, which can be generated within minutes in the initiation phase of inflammation following the recruitment of neutrophils. Data from our study supports the hypothesis that PGs may also participate in this EIU inflammatory process.

Lysophospholipids have been proven to be generated during stress, injury, or apoptosis. They are also known as signaling lipids that can modulate immune responses by influencing various leukocytes, including neutrophils and macrophages^[6-7,26-30]. Within this class, LysoPC has been clinically found to show the local and systemic level increase in certain inflammatory diseases such as atherosclerosis^[31-32], and has been experimentally considered to modulate neutrophil and macrophage activation, and mediate phagocytic clearance of apoptotic cells^[5-8]. In our animal model, we detected a significant increase in LysoPC in the EIU AH and retina compared to that in the control group (Figures 5A and 9A), along with massive neutrophil aggregation in the anterior chamber and less aggregation in the vitreous (Figures 2C and 2D). These results indicated that LysoPC might have participated in neutrophil activation and trafficking in this acute inflammation model. Several specific LysoPCs, such as 18:0 LysoPC, have been reported to activate G protein-coupled receptor G2A-mediated leukocyte response, which serves as a protective factor^[33]. In our study, we found a noteworthy increase in 18:0 LysoPC (fold change=6.4 in the AH and 3.8 in the retina) in the EIU group, indicating that enhanced level of 18:0 LysoPC might play an important role in this EIU inflammatory process. The higher quality ratio of LysoPC/PC that has been hypothesized to be a reliable indicator of rheumatoid arthritis and multiple sclerosis in early stages^[34-35] was also found in the EIU AH and retina. This reminds us that the LysoPC/PC ratio might be used as a local indicator of EIU occurrence.

In addition to LysoPC, other lysophospholipids may also serve as signaling lipids that can affect leukocyte function^[6]. LysoPS generated in activated or apoptotic neutrophils promotes their lymphatic clearance by macrophages^[7,36]. This function of LysoPS is believed to be critical for the resolution of inflammation and tissue restoration. From our investigation of the EIU model, in the acute inflammation phase, the relative intensity level of LysoPS noticeably decreased in the EIU AH compared to that in the control AH (fold change =0.37),

and the quality ratio of LysoPS/PS was 80% in EIU, which was identical to the value of 79% found in the control AH. Simultaneously, massive amount of neutrophils were observed in the anterior chamber. In contrast, the relative intensity level of LysoPS was increased in the EIU retina by 3.6-fold higher than in the control retina, and the quality ratio of LysoPS/PS was 28% in the EIU retina, which was slightly higher than that (25%) found in the control retina. In particular, 18:0 and 18:1 LysoPS, already known as bioactive signaling phospholipids and abundant modified PS species following activation of the neutrophil oxidase, showed a significant increase in the EIU retina compared to that in the control retina, with fold changes of 2.9 and 1.6, respectively, while they were absent in the EIU and control AH. On the basis of the histological results (Figure 2C and 2D), very few neutrophils were observed in the retina than in the AH. Taken together, we found a negative correlation between LysoPS expression and leukocyte aggregate. We conjectured that LysoPS might participate in the resolution of inflammation and topical application of LysoPS in AH might enhance the phagocytosis of apoptotic neutrophils and promote the tissue restoration.

Increasing understanding gained in sphingolipid metabolism has revealed that certain sphingolipid metabolites, especially ceramide can serve as a bioactive messenger in initiating and modulating inflammation and inflammatory disorders^[37]. Ceramide can be yielded from sphingomyelins produced by the first enzyme in the sphingolipid de novo biosynthetic pathway, serine palmitoyltransferase, which may be upregulated by pro-inflammatory cytokines such as IL-1 and TNF- α . After ceramide is produced, a series of pathways such as the PP2A/Akt pathway is triggered to promote the generation of downstream pro-inflammatory cytokines and enhance immune cell trafficking and inflammation responses^[38]. Ceramide metabolism pathways can also yield other bioactive sphingolipids that can regulate inflammation. In one pathway it could be phosphorylated by ceramide kinase (CERK) to form C-1-P, an important bioactive signaling molecule that can modulate cell growth and survival and particularly play an important role in inflammation and homeostasis restoration^[39-42]. In our investigation, the relative intensity analysis showed that the amount of total sphingolipids in the EIU AH was slightly higher than those in the control AH (fold change =1.2). A further study demonstrated that Cer240, Cer241, and SM240 were remarkably increased in the EIU AH, with fold changes 1.6, 9.0, and 2.0, respectively. The expression of IL-6 and TNF- α was also dramatically elevated in the EIU AH compared to that in the control AH ($P<0.05$; Figure 1C). On the basis of the former theories, we conjectured that TNF- α might have triggered an upregulation of serine palmitoyltransferase and promoted the production of sphingomyelin. Subsequently sphingomyelin underwent

metabolic transformation to ceramide, which led to the increase in ceramide amount in the EIU AH, consequently leading to accumulation of a massive amount of neutrophils. Concurrently, the amount of total sphingolipids also significantly increased in the EIU retina by 2.8-fold, especially with increased levels of C12 C-1-P, C16 C-1-P, and C24 C-1-P and upregulation of Cer160, Cer240, SM120, and SM240. Several endogenous C-1-P studies have shown that endotoxin stimulated macrophages showed increased levels of C24:1 C-1-P in just 30mins after stimulation, and even multiple C-1-P species were observed over an 8- to 24-h period^[43]; this finding is similar to our observation. The evidence derived from the experimental studies of exogenous C-1-P administration reveals that C-1-P may exert this effect by inhibiting NF- κ B activation and consequently decreasing the secretion of pro-inflammatory factors^[40]. In our study, LPS administration upregulated the C-1-P amount, while elevated NF- κ B was found in the EIU retina (Figure 1D and 1E). Enhancement of endogenous C-1-P was believed to be unable to reverse the inflammation process induced by LPS.

Taken together, in this EIU model, we found that a variety of inflammation regulating lipids showed changes in the amount and conjectured that these lipids played important roles in this inflammation process. Exogenous topical application of these protective lipids or inhibition of these pro-inflammatory lipids may be useful therapeutic strategies for the resolution of EIU inflammation. The underlying mechanism also warrants further studies.

ACKNOWLEDGEMENTS

We thank Kun Liu and Qing Gu for their excellent technical support.

Foundations: Supported by the National Natural Science Foundation of China (No.81300776); the Youth Scientific Research Project of Shanghai Municipal Health Bureau (No.20134Y088).

Conflicts of Interest: Wang HY, None; Wang Y, None; Zhang Y, None; Wang J, None; Xiong SY, None; Sun Q, None.

REFERENCES

- 1 Reeves SW, Sloan FA, Lee PP, Jaffe GJ. Uveitis in the elderly: epidemiological data from the National Long-term Care Survey Medicare Cohort. *Ophthalmology* 2006;113(2):307.
- 2 Adán-Civera AM, Benítez-Del-Castillo JM, Blanco-Alonso R, Pato-Cour E, Sellas-Fernández A, Bañares-Cañizares A. Burden and direct costs of non infectious uveitis in Spain. *Reumatol Clin* 2016;12(4):196-200.
- 3 Prete M, Dammacco R, Fatone MC, Racanelli V. Autoimmune uveitis: clinical, pathogenetic, and therapeutic features. *Clin Exp Med* 2016;16(2):125-136.
- 4 Antony P, Baby B, Vijayan R. Molecular insights into the binding of phosphoinositides to the TH domain region of TIPE proteins. *J Mol Model* 2016;22(11):272.

- 5 Radu CG, Yang LV, Riedinger M, Au M, Witte ON. T cell chemotaxis to lysophosphatidylcholine through the G2A receptor. *Proc Natl Acad Sci U S A* 2004;101(1):245-250.
- 6 Frasch SC, Zemski-Berry K, Murphy RC, Borregaard N, Henson PM, Bratton DL. Lysophospholipids of different classes mobilize neutrophil secretory vesicles and induce redundant signaling through G2A. *J Immunol* 2007;178(10):6540-6548.
- 7 Frasch SC, Berry KZ, Fernandez-Boyanapalli R, Jin HS, Leslie C, Henson PM, Murphy RC, Bratton DL. NADPH oxidase-dependent generation of lysophosphatidylserine enhances clearance of activated and dying neutrophils via G2A. *J Biol Chem* 2008;283(48):33736-33749.
- 8 Chen G, Li J, Qiang X, Czura CJ, Ochani M, Ochani K, Ulloa L, Yang H, Tracey KJ, Wang P, Sama AE, Wang H. Suppression of HMGB1 release by stearyl lysophosphatidylcholine: an additional mechanism for its therapeutic effects in experimental sepsis. *J Lipid Res* 2005;46(4):623-627.
- 9 Kunisawa J, Kiyono H. Sphingolipids and epoxidized lipid metabolites in the control of gut immunosurveillance and allergy. *Front Nutr* 2016;3:3.
- 10 Ghidoni R, Caretti A, Signorelli P. Role of sphingolipids in the pathobiology of lung inflammation. *Mediators Inflamm* 2015;2015:487508.
- 11 Rivera J, Proia RL, Olivera A. The alliance of sphingosine-1-phosphate and its receptors in immunity. *Nat Rev Immunol* 2008;8(10):753-763.
- 12 Lajavardi L, Bochot A, Camelo S, Goldenberg B, Naud MC, Behar-Cohen F, Fattal E, de Kozak Y. Downregulation of endotoxin-induced uveitis by intravitreal injection of vasoactive intestinal Peptide encapsulated in liposomes. *Invest Ophthalmol Vis Sci* 2007;48(7):3230-3238.
- 13 Lou Y, Liu S. The TIPE (TNFAIP8) family in inflammation, immunity, and cancer. *Mol Immunol* 2011;49(1-2):4-7.
- 14 Oberoi R, Schuett J, Schuett H, Koch AK, Luchtfeld M, Grote K, Schieffer B. Targeting tumor necrosis factor- α with Adalimumab: effects on endothelial activation and monocyte adhesion. *PLoS One* 2016;11(7):e0160145.
- 15 Chu CJ, Gardner PJ, Copland DA, Liyanage SE, Gonzalez-Cordero A, Kleine Holthaus SM, Luhmann UF, Smith AJ, Ali RR, Dick AD. Multimodal analysis of ocular inflammation using the endotoxin-induced uveitis mouse model. *Dis Model Mech* 2016;9(4):473-481.
- 16 Shen W, Gao Y, Lu B, Zhang Q, Hu Y, Chen Y. Negatively regulating TLR4/NF- κ B signaling via PPAR α in endotoxin-induced uveitis. *Biochim Biophys Acta* 2014;1842(7):1109-1120.
- 17 Mérida S, Sancho-Tello M, Navea A, Almansa I, Muriach M, Bosch-Morell F. An anti-interleukin-2 receptor drug attenuates T-helper 1 lymphocytes-mediated inflammation in an acute model of endotoxin-induced uveitis. *PLoS One* 2014;9(3):e90216.
- 18 Smith JR, Hart PH, Williams KA. Basic pathogenic mechanisms operating in experimental models of acute anterior uveitis. *Immunol Cell Biol* 1998;76(6):497-512.
- 19 Okumura A, Mochizuki M. Endotoxin-induced uveitis in rats: morphological and biochemical study. *Jpn J Ophthalmol* 1988;32(4):457-465.
- 20 Behar-Cohen FF, Savoldelli M, Parel JM, Goureau O, Thillaye-Goldenberg B, Courtois Y, Pouliquen Y, de Kozak Y. Reduction of corneal edema in endotoxin-induced uveitis after application of L-NAME as nitric

- oxide synthase inhibitor in rats by iontophoresis. *Invest Ophthalmol Vis Sci* 1998;39(6):897-904.
- 21 Bligh EG, Dyer WJ. A rapid method of total lipid extraction and purification. *Can J Biochem Physiol* 1959;37(8):911-917.
- 22 Aribindi K, Guerra Y, Lee RK, Bhattacharya SK. Comparative phospholipid profiles of control and glaucomatous human trabecular meshwork. *Invest Ophthalmol Vis Sci* 2013;54(4):3037-3044.
- 23 Yang K, Cheng H, Gross RW, Han X. Automated lipid identification and quantification by multidimensional mass spectrometry-based shotgun lipidomics. *Anal Chem* 2009;81(11):4356-4368.
- 24 Sun H, Gong S, Carmody RJ, Hilliard A, Li L, Sun J, Kong L, Xu L, Hilliard B, Hu S, Shen H, Yang X, Chen YH. TIPE2, a negative regulator of innate and adaptive immunity that maintains immune homeostasis. *Cell* 2008;133(3):415-426.
- 25 Kosinska MK, Liebisch G, Lochnit G, Wilhelm J, Klein H, Kaesser U, Lasczkowski G, Rickert M, Schmitz G, Steinmeyer J. Sphingolipids in human synovial fluid—a lipidomic study. *PLoS One* 2014;9(3):e91769.
- 26 Müller J, Petković M, Schiller J, Arnold K, Reichl S, Arnhold J. Effects of lysophospholipids on the generation of reactive oxygen species by fMLP- and PMA-stimulated human neutrophils. *Luminescence* 2002;17(3):141-149.
- 27 Lin P, Welch EJ, Gao XP, Malik AB, Ye RD. Lysophosphatidylcholine modulates neutrophil oxidant production through elevation of cyclic AMP. *J Immunol* 2005;174(5):2981-2989.
- 28 Kabarowski JH. G2A and LPC: regulatory functions in immunity. *Prostag Oth Lip M* 2009;89(3-4):73-81.
- 29 Frasch SC, Fernandez-Boyanapalli RF, Berry KA, Murphy RC, Leslie CC, Nick JA, Henson PM, Bratton DL. Neutrophils regulate tissue Neutrophilia in inflammation via the oxidant-modified lipid lysophosphatidylserine. *J Biol Chem* 2013;288(7):4583-4593.
- 30 Frasch SC, Fernandez-Boyanapalli RF, Berry KZ, Leslie CC, Bonventre JV, Murphy RC, Henson PM, Bratton DL. Signaling via macrophage G2A enhances efferocytosis of dying neutrophils by augmentation of Rac activity. *J Biol Chem* 2011;286(14):12108-12122.
- 31 Kurien BT, Scofield RH. Lipid peroxidation in systemic lupus erythematosus. *Indian J Exp Biol* 2006;44(5):349-356.
- 32 Matsumoto T, Kobayashi T, Kamata K. Role of lysophosphatidylcholine (LPC) in atherosclerosis. *Curr Med Chem* 2007;14(30):3209-3220.
- 33 Jackson SK, Abate W, Tonks AJ. Lysophospholipid acyltransferases: novel potential regulators of the inflammatory response and target for new drug discovery. *Pharmacol Ther* 2008;119(1):104-114.
- 34 Fuchs B, Schiller J, Wagner U, Häntzschel H, Arnold K. The phosphatidylcholine/lysophosphatidylcholine ratio in human plasma is an indicator of the severity of rheumatoid arthritis: investigations by 31P NMR and MALDI-TOF MS. *Clin Biochem* 2005;38(10):925-933.
- 35 Del Boccio P, Pieragostino D, Di Ioia M, Petrucci F, Lugaresi A, De Luca G, Gambi D, Onofri M, Di Ilio C, Sacchetta P, Urbani A. Lipidomic investigations for the characterization of circulating serum lipids in multiple sclerosis. *J Proteomics* 2011;74(12):2826-2836.
- 36 Frasch SC, Bratton DL. Emerging roles for lysophosphatidylserine in resolution of inflammation. *Prog Lipid Res* 2012;51(3):199-207.
- 37 Chan C, Goldkorn T. Ceramide path in human lung cell death. *Am J Respir Cell Mol Biol* 2000;22(4):460-468.
- 38 Maceyka M, Spiegel S. Sphingolipid metabolites in inflammatory disease. *Nature* 2014;510(7503):58-67.
- 39 Hannun YA, Obeid LM. Principles of bioactive lipid signalling: lessons from sphingolipids. *Nat Rev Mol Cell Biol* 2008;9(2):139-150.
- 40 Hankins JL, Fox TE, Barth BM, Unrath KA, Kester M. Exogenous ceramide-1-phosphate reduces lipopolysaccharide (LPS)-mediated cytokine expression. *J Biol Chem* 2011;286(52):44357-44366.
- 41 Shirey CM, Ward KE, Stahelin RV. Investigation of the biophysical properties of a fluorescently modified ceramide-1-phosphate. *Chem Phys Lipids* 2016;200:32-41.
- 42 Granado MH, Gangoiti P, Ouro A, Arana L, Gómez-Muñoz A. Ceramide 1-phosphate inhibits serine palmitoyltransferase and blocks apoptosis in alveolar macrophages. *Biochim Biophys Acta* 2009;1791(4):263-272.
- 43 Józefowski S, Czerkies M, Łukasik A, Bielawska A, Bielawski J, Kwiatkowska K, Sobota A. Ceramide and ceramide 1-phosphate are negative regulators of TNF- α production induced by lipopolysaccharide. *J Immunol* 2010;185(11):6960-6973.